Corrosion resistance of CrN PVD coatings: comparison among different deposition techniques

L. Montesano, M. Gelfi, A. Pola, P. Colombi, G.M. La Vecchia

Corrosion resistance of CrN PVD coatings were evaluated with polarization tests in NaCl and HCl environment. The effect of the deposition technique and the related defects morphology were studied and corrosion mechanisms were evaluated on the basis of the detected defects type.
It was found that the presence of two layers in coating architecture delays corrosion; this solution is a good advice in designing coatings for applications where good corrosion resistance is required.
Coating porosity, calculated using two different models available in literature, was compared with experimental evidences. Formulas based on polarization resistance are in agreement with morphological SEM analyses but, on the contrary, mixed potential model appears not suitable for coating porosity calculation.

Keywords: PVD coatings, corrosion

INTRODUCTION

One of the main cause of failure of coated components is related to corrosive phenomena starting from deposition defects such as areas with excessive low thickness due to complex part shape or errors during the deposition process [1-3].
In many applications coatings are present also as finishing; in these cases, it is important to guarantee coating resistance in the working environment because its damaging can decrease surface properties and causes inefficiency of the component.
To gain this property, one way consists in studying the best combination of substrate and coating; on the other hand, it is fundamental to understand which is the minimum coating thickness able to assure a good corrosion protection, taking into account the different aggressive environmental conditions. In order to improve coating resistance, it can be also useful to consider different deposition techniques, coating design (in terms of number and chemical composition of each layer that compose the whole thickness) and quantity and type of defects that surely act as preferential corrosion sites.
As an example, polymers injection moulding dies undergo wear, due to the presence of hard particles in the plastic matrix, and corrosion related to the presence of chemical aggressive species like chlorine, fluorine or sulfur that can be released during the process [4].
The use of a thin ceramic coating can solve these problems because of its higher hardness and lower chemical reactivity compared with the bare steel.
For these reasons, the real benefits of coatings in increasing die life must be well understood for a reliable use in industrial applications. Laboratory tests result very important to discern coating behavior, although they often are not well-related to the real working conditions because of the complex state of mechanical and thermic stress affecting a die. Therefore, specific tests are needed in order to simulate the real working conditions and to understand the changes that the use of a coating induces on the components.
In this work it is presented a preliminary study on corrosion performance of CrN PVD coatings. Potenziodynamic tests performed in NaCl and HCl were carried out in order to simulate dies working conditions in plastic injection moulding. Chloride ions and acid condition can be present during this process both for gas release and vapor condensation on dies surface and, for this reason, the coating has to be chosen considering also its pitting corrosion resistance. Tested samples were coated using DC magnetron sputtering and cathodic arc erosion and combining the two techniques; monolayered and double layered coatings were produced maintaining a constant thickness.
Scanning electronic microscope equipped with EDS probe was used to analyze the samples' surface and cross sections before and after corrosion tests to understand corrosive mechanism as a function of the coating detected defects.

L. Montesano, M. Gelfi, A. Pola, G.M. La Vecchia
DIMI, Università di Brescia

P. Colombi
CSMT Gestione Scarl, Brescia

C [%]	S [%]	P [%]	Mn [%]	Cr [%]	Ni [%]	Mo [%]	Cu [%]	Si [%]	Al [%]
0,28	0,002	0,008	0,62	0,85	3,06	0,51	0,17	0,31	0,023

Table I: Chemical composition of the used substrate.

Tabella I: Composizione chimica dell'acciaio utilizzato.

EXPERIMENTAL PROCEDURE

All the investigated coatings were deposited on a tool steel whose chemical composition is reported in Table I.
The specimens were machined from a steel plate (4 mm in thickness) in order to obtain disks with a diameter of 18mm. All the samples were ground and polished up to mirror finish, cleaned with ethanol and dried before coating deposition.
Five different sets of samples were considered and named as follows:

A) Steel substrate without any coating;
B) CrN single layer deposited by DC magnetron sputtering (MS) with a total thickness of 4 microns;
C) CrN double layer deposited by DC-MS technique using the same parameters of coating B in order to obtain the first layer (2 microns); then the process was interrupted, the sample was taken out form the vacuum chamber, cleaned with ethanol and subsequently coated with other 2 microns, without changing any parameter.
D) CrN double layer deposited by cathodic arc evaporation (CAE). The deposition was interrupted between the two layers. A soft shot-peening was carried out in order to remove the droplets on the surface of the first CrN layer and to promote the adhesion with the second one. A total coating thickness of 4 microns was obtained.
E) CrN double layer obtained mixing the two techniques: the first layer was deposited by CAE and the second one by DC-MS. Deposition parameters were the same used for deposition of coatings B and D.

In Table II the studied coatings and used deposition techniques are summarized.

Coating thickness was evaluated by calotest measurements.
Corrosion resistance was studied by means of electrochemical polarization tests performed with AMEL 7050 potenziostat, using as aggressive environment both 3.5%wt NaCl and 0.1M HCl aqueous solution. These environments contain chloride (Cl^-) and are suitable to investigate samples pit tendency. Their different pH allows also to simulate different working conditions.
All the performed tests were carried out at room temperature and at a potential between -0.8 and +1.5mV (SCE), with a scanning rate of 0.25mV/s. This wide potential range was chosen in order to study free corrosion (E_0 and i_0) and also passivation phenomena.
Each test started 30 minutes after the sample immersion in the solution, in order to reach a constant free corrosion potential.
E_0 and i_0 were extrapolated from polarization curves by Tafel method, while polarization resistance, Rp and porosity level, P were calculated according to the following formulae:

$$Rp = \frac{\beta_a \times \beta_c}{2.3039(\beta_a + \beta_c) \times i_0} \quad [3] \quad (1)$$

where βa and βc are respectively the anodic and cathodic Tafel slopes, and i_0 is the corrosion current density, and

$$P = \left(\frac{Rp_{substrate}}{Rp_{coating}}\right) \times 10^{\frac{-|\Delta E_0|}{\beta a}} \quad [3, 5] \quad (2)$$

where R_p is the polarization resistance, ΔE_0 is the differen-

Coating	First layer	Second layer	Total thickness
A: none	XXX	XXX	XXX
B: mono layered MS	4 µm DC - MS	XXX	4 µm
C: double layered MS	2 µm DC - MS	2 µm DC - MS	4 µm
D: double layered CAE	2 µm CAE	2 µm CAE	4 µm
E: double layered CAE + MS	2 µm CAE	2 µm DC - MS	4 µm

Table II: Studied coatings

Tabella II: Rivestimenti analizzati

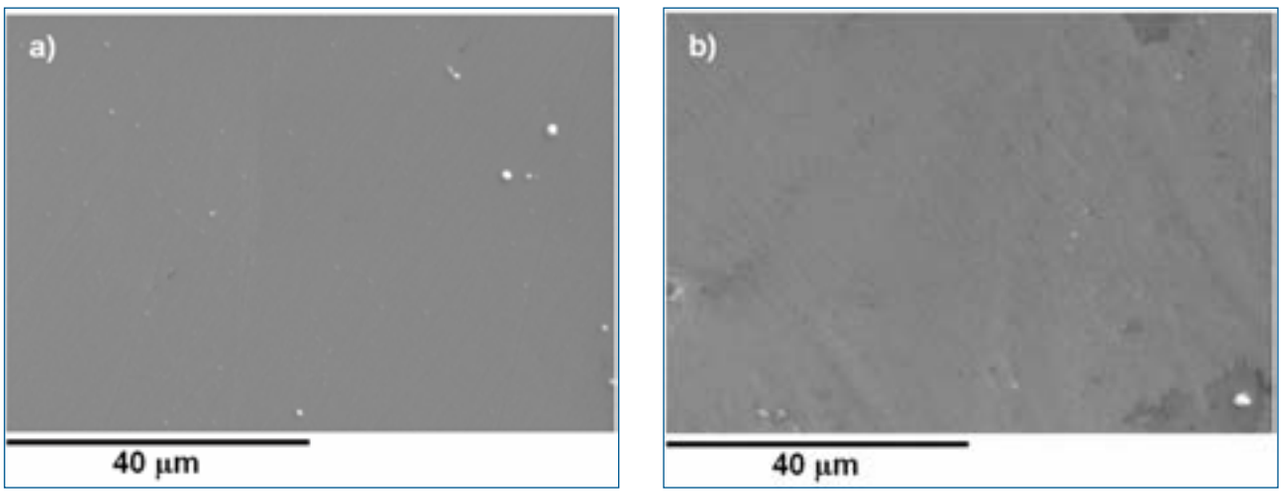

Fig. 1: DC magnetron sputtering coatings: monolayer B (a), and double layer C (b)

Fig. 1: Rivestimenti DC magnetron sputtering: coating monostrato B (a) e doppio strato C (b)

ce between substrate and coating corrosion potential, and β_a is the substrate anodic curve slope.
Coating porosity was also calculated by using the mixed potential theory E_m: under the assumption that, for low potential, the coating does not corrode due to his higher nobility than steel, the corrosion potential of the sample (E_m) is given by the equation:

$$E_m = E^A_{corr} + \beta_a \log\left(\frac{Sc}{Sa}\right) \quad [6] \ (3)$$

where E^A_{corr} and βa are respectively the corrosion potential and the Tafel slope of the anodic element (substrate) and S_c/S_a is the surface ratio between cathodic and anodic areas [6]. Assuming that cathodic areas are mainly localized on the bottom of the coating defects, porosity level becomes $\frac{1}{Sc/Sa}$.

Morphological characterizations and semi-quantitative chemical analysis of the coatings were performed by Leo Evo 40 scanning electron microscope (SEM) equipped with Energy Dispersive Spectroscopy Probe (EDS). All the data reported in the spectra are in weight %. Both surface and cross section were analyzed to verify the presence of deposition defects in order to study their morphology, size and distribution as well as growth along the layer thickness.

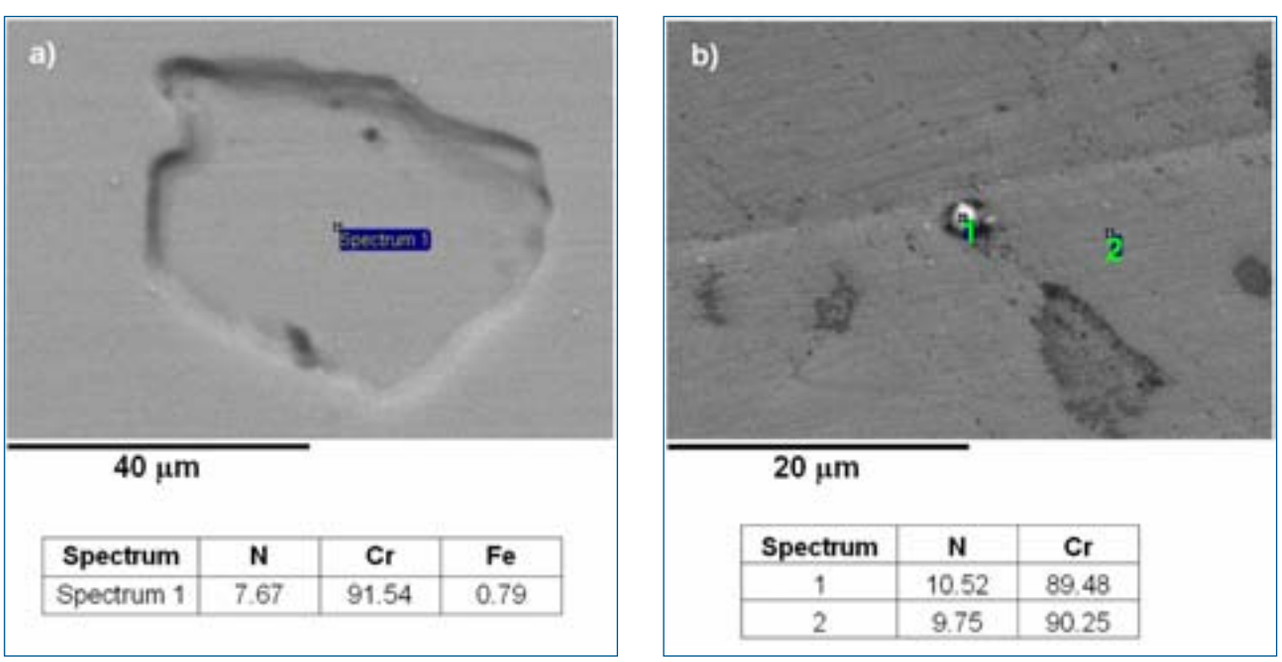

Spectrum	N	Cr	Fe
Spectrum 1	7.67	91.54	0.79

Spectrum	N	Cr
1	10.52	89.48
2	9.75	90.25

Fig. 2 Coating B: examples of cavities and droplets

Fig. 2 Dettaglio del rivestimento B: esempio di cavità e di droplet

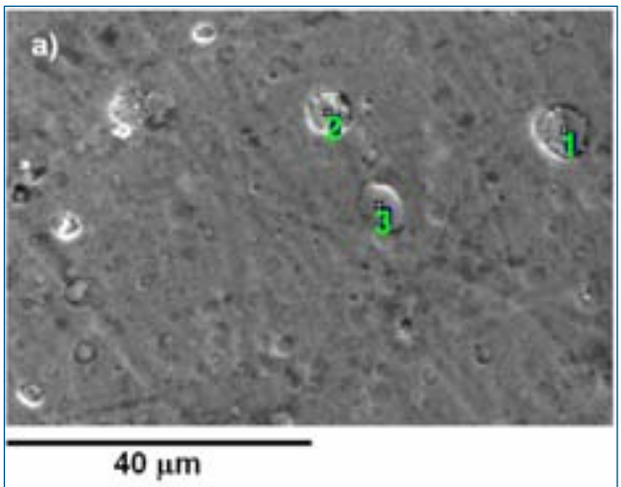

Spectrum	N	O	Cr
1		4.88	95.12
2	4.29	7.01	88.70
3			100.00

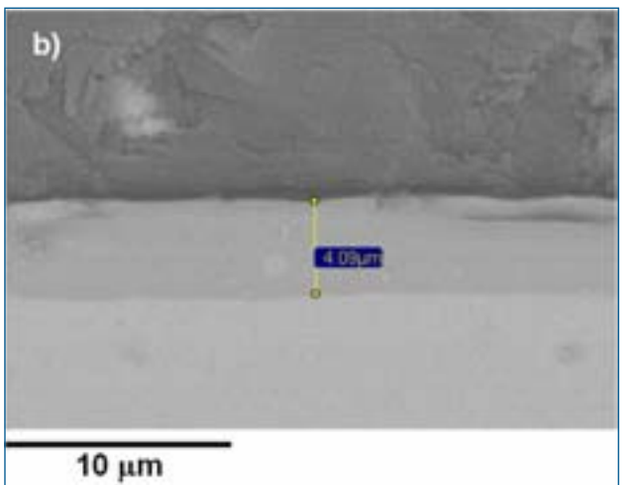

Fig. 3 Coating D (double layer Cathodic Arc Evaporation) surface view (a), and cross section view (b)

Fig. 3 rivestimento D (doppio strato Cathodic Arc Evaporation) in superficie (a) e in sezione (b)

RESULTS

Analyses on "as deposited" samples

Figure 1 shows surface morphology for coating B and C. It can be seen that coatings obtained by DC-MS (B and C) are characterized by a good superficial aspect and a low amount of defects on the surfaces.

Two types of defects were detected analyzing the coatings surface: cavities (Fig. 2a) and droplets (Fig. 2b, spectrum 1).

Such defects are originated during deposition if the vacuum chamber is not clean. In fact, dust particles or CrN powder present on the chamber walls can lay on the sample surface and determinate an abnormal growth of the coating with a gradient of stresses. The higher the thickness the higher the stresses that can, in some cases, induce coating delamination [3, 7].

EDS analyses in Fig. 2 indicate that the chemical composition of these defects is the same of that of the coating, both

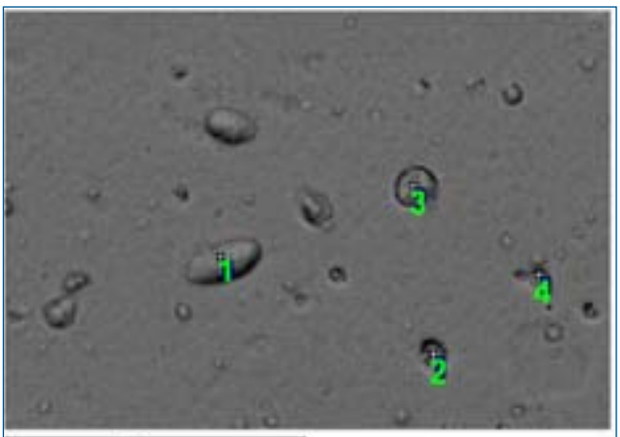

Spectrum	N	Cr
1	11.54	88.46
2	8.30	91.70
3	8.40	91.60
4	8.11	91.89

Fig. 4: Coating E (double layer CAE and Sputter)

Fig. 4: rivestimento E (doppio strato CAE e Sputter)

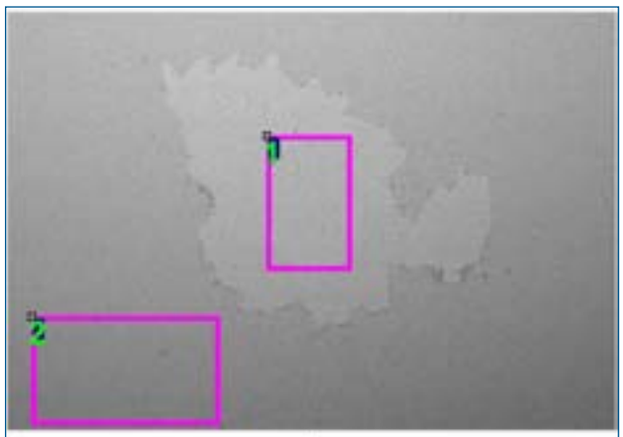

Spectrum	N	Cr
1	13.22	86.78
2	11.01	88.99

Fig.5: Coating E; example of detachment defect related to the weak adhesion between the first and second layer

Fig.5: Particolare del rivestimento E; esempio di difetto riconducibile a scarsa adesione tra i due strati di rivestimento

in the case of both cavities and droplets. However, these areas should represent preferential corrosion sites being coated areas with lower thickness. SEM analyses, performed on cross section, show a good adhesion between coating and steel; no areas without coating or porosity that connect substrate and external environment were detected.
Fig. 3 presents some SEM images of the coating D (deposited by CAE technique). Its surface is not smooth like MS coating but many defects are uniformly present on the sample. Cross sectional images show a good adhesion for this coating too. Defects morphologies are the same of coating B and C but their origins are different. In this case, in fact, droplets are of metallic chromium (Fig. 3a) that came from the Cr target used during deposition. Cavities have spherical shape that, most likely, previously had droplets inside, or they can be related to abnormal growth of the coating due to the presence of pollutant particles in the deposition chamber [7, 8]. Defect size covers a wide range , starting from hundreds of nanometers to microns.
Looking at coating E micrographs, it is possible to asses that the combination of the two techniques permits the obtainment of samples with a defects concentration similar to that of coating CAE (Fig. 4). To understand their origin, higher magnification observations were carried out. They can be divided in two categories:

- Droplets generate during the first layer deposition (CAE), then covered by the second layer (MS). EDS analysis shows that on the sample's surface a CrN layer is present that covers the imperfections of the lower layer;
- Delaminations between the two layers, similar to those present on B and C samples' surface. These defects size can be of some microns or significantly higher, like that measured in Fig. 5. This rupture can be caused by the presence of Cr droplets deposited in the CAE layer. In fact, these droplets can modify the residual stress of the MS coating, causing the detachment of the superior layer where residual stresses are higher.

Corrosion tests in NaCl

Fig. 6 shows polarization curves of the different analyzed coatings and for the bare steel. As expected, the worst behavior is that of the substrate (it shows the higher i_0 and the lower E_0); all the coatings exhibit a protective effect, independently of the PVD deposition technique. However, results show that deposition technique and number of layers modify coating behavior in the corrosive environment.

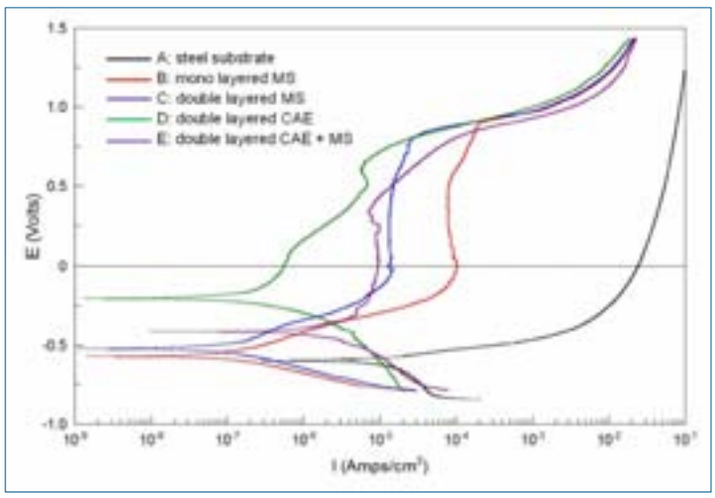

Fig. 6: Polarization curves in NaCl 3.5%wt acqueous solution

Fig. 6: Prove di corrosione di polarizzazione elettrochimica in NaCl

Coatings B and C (obtained by MS) shows a low current density and a pseudo-passive region between 0 and +900mV, but their free corrosion potential is clearly lower than that of coating D (CAE).
The coating E behavior is between the CAE and the MS coating: E_0 is higher than in the case of sputtered coatings but lower than that of cathodic arc one; a passive region is present but its extension is lower and it starts from lower potential (from -250mV to 250mV) than that of the MS coating. However, the use of the second layer increases corrosion resistance which is higher than that of the mono layered.
Table III shows corrosion tests results in NaCl solution as the mean value of, at least, three tests. Current density and free corrosion potential were extrapolated directly from polarization curves using Tafel method, while polarization resistance (Rp) and porosity level (P) were calculated by using

Coating	i_0 [A/cm^2]	E_0 [V]	Rp [Ohm]	P	P [Em]
A: none	7.8E-06	-0.601	2.5E+03	100.00%	100.00%
B: mono layered MS	1.2E-07	-0.572	2.4E+05	0.38%	36.43%
C: double layered MS	1.1E-07	-0.546	3.3E+05	0.14%	18.60%
D: double layered CAE	8.2E-07	-0.326	2.0E+05	0.01%	0.11%
E: double layered CAE + MS	2.0E-06	-0.412	4.6E+04	0.01%	0.12%

Table III: Results of corrosion test in NaCl 3.5%wt solution

Tabella III: Risultati delle prove di corrosione in NaCl 3.5%

(1) - (2) - (3) formulae. It can be clearly seen that the different methods used in the porosity level calculations give different results. Mixed potential model assesses that porosity level for MS coating is extremely high, in some case higher than 30%, and this value appears not realistic, considering coating morphology and SEM observations. These results are also in contrast with the measured low current density.
Porosity calculated from polarization resistance (Formula 2), on the other hand, are more realistic: values are low and in agreement with SEM analyses. In particular, due to a higher density than MS coating, CAE sample shows a lower porosity level; its corrosion current density is higher and this apparently disagrees with calculated porosity level. However, it can be seen in polarization curves that the CAE cathodic branch shifts to higher current values than those of coating B and C. This suggests that cathodic processes are more efficient on its surface. It can be concluded that corrosion can occur rapidly but only in the few areas on the bottom of the porosity. This modification in the cathodic processes is probably related to the presence of metallic droplets that act as cathodic areas, shifting free corrosion potential to higher values.
Comparing the coatings obtained with the same technique (B and C), a good correlation between porosity level and corrosion current density can be found: Rp decreases and i_0 grows as porosity level increases.
Notwithstanding its low porosity level, coating E, obtained with the combination of both the techniques, exhibits large areas with the detachment of the upper layer in which the coating is thinner than elsewhere. As a consequence, a weak protective effect is observed; Rp resulted an order of magnitude lower than that of other coatings and its corrosion current density in between bare steel and the other tested coatings.
SEM analyses performed after corrosion tests showed pit formation on the MS sample surface (Fig. 7a). Such defects are able to reach, for the monolayered, the substrate that appears corroded below the coating. In the case of the double layered, on the other hand, some ruptures at the interface between the two layers can be detected and the upper part of the coatings is not present in many areas. In the CAE sample (D) only metallic chromium droplets are corroded as reported in other literature works [9] (Fig. 7b). This different behaviour can explain the presence of the passivity region present only in the MS deposited coating polarization curves. During the tests corrosion products fill the porosity present in the coating and the corrosion rate slows down [10]. For B and C coatings, as it can be seen in the polarization curves, the current density needed to reach passivation region is related to the calculated porosity level. Deposits formation, that can occlude coating pores, is proportional to the metallic ions formation and, therefore, to the current density. Coating B (monolayer) is characterized by a higher porosity level respect to the double layered one (C); in fact, a higher current density is required to have a sufficient amount of corrosion products to reach the passive state. As this situation is achieved, current density remains almost constant since the potential increase up to a sufficiently high value that causes CrN rupture. For higher values (more than +900mV) corrosive solution can reach and damage the substrate that appears corroded underneath the coating. In some areas deposits

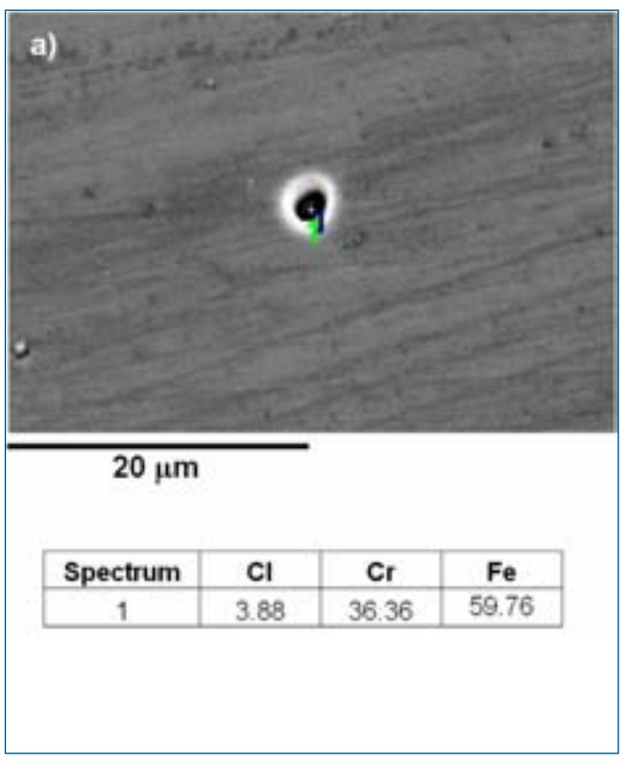

Spectrum	Cl	Cr	Fe
1	3.88	36.36	59.76

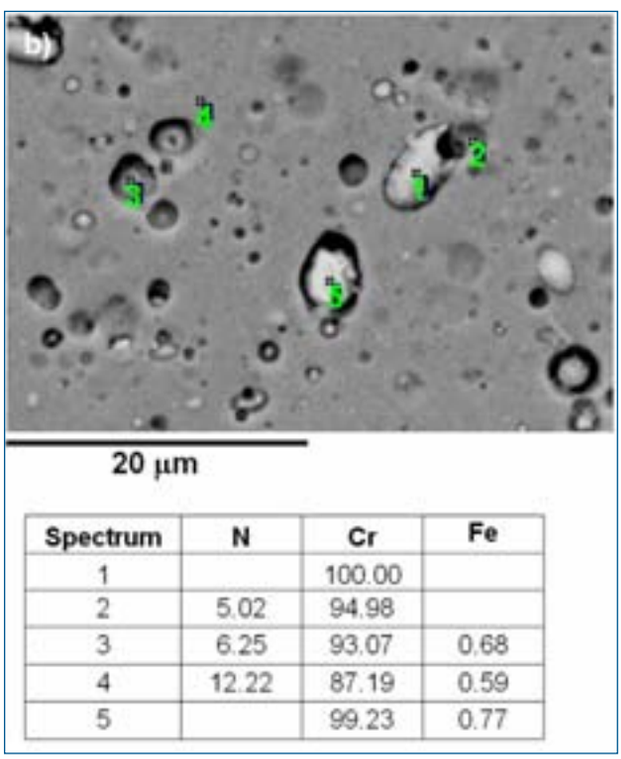

Spectrum	N	Cr	Fe
1		100.00	
2	5.02	94.98	
3	6.25	93.07	0.68
4	12.22	87.19	0.59
5		99.23	0.77

Fig.7: Corrosion morphology: coating B (a) and coating D (b)

Fig.7: Esempi di corrosione dei coating B (a) e del coating D (b)

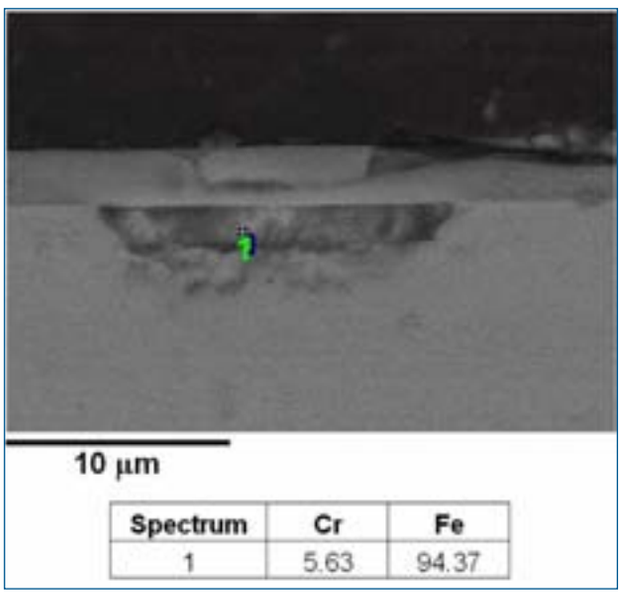

Fig. 8: Coating B: corrosion morphology

Fig. 8: Morfologia di corrosione per il coating B

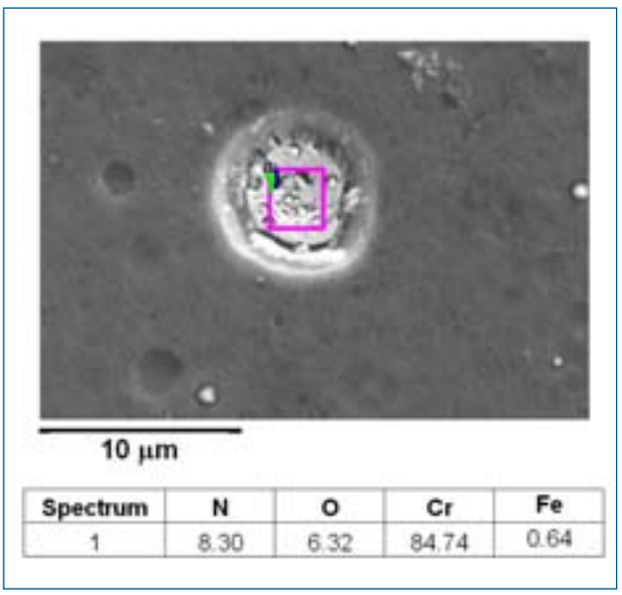

Fig. 9: Coating E: corrosion morphology

Fig. 9: Morfologia di corrosione per il coating E

formation tends to lift the coating and to produce delaminations, leaving the steel exposed to the environment (Fig. 8). In CAE deposited samples current density grows continuously increasing potential but it remains lower than that recorded for the other coatings.

Finally, coating E, obtained by both the techniques (CAE + MS), shows a corrosion morphology in between CAE and MS samples: on the droplet surfaces they are present both ruptures of the MS layer and droplet corrosion phenomenon (Fig. 9). This process doesn't reach the substrate and, in fact, no corrosion sites connected with the steel were detected.

Corrosion tests in HCl

Polarization tests in HCl 0.1M show a higher increase in corrosion resistance than in the case of NaCl test, due to the presence of the coatings (Fig. 10). Free corrosion potentials of coated samples are similar to those of bare steel and nobler than potentials measured in NaCl, as found also by other Authors [4, 11].

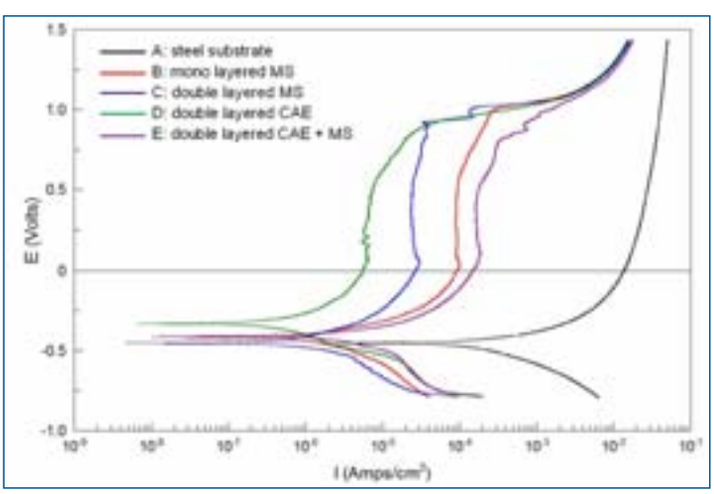

Fig. 10: Polarization curves in HCl 0.1M acqueous solution

Fig. 10: Prove di corrosione di polarizzazione in HCl 0.1M

Coating	i0 [A/cm²]	E0 [V]	Rp [Ohm]	P	P [Em]
A: none	5.31E-04	-0.439	1.4E+02	100.00%	100.00%
B: mono layered MS	9.54E-07	-0.419	2.6E+04	0.42%	75.91%
C: double layered MS	5.64E-07	-0.454	3.5E+04	0.33%	123.65%
D: double layered CAE	1.90E-07	-0.362	7.3E+04	0.19%	46.64%
E: double layered CAE + MS	1.32E-06	-0.401	1.5E+04	0.60%	59.58%

Table IV: Results of corrosion tests in HCl 0.1M solution

Tabella IV: Risultati delle prove di corrosione in HCl 0.1M.

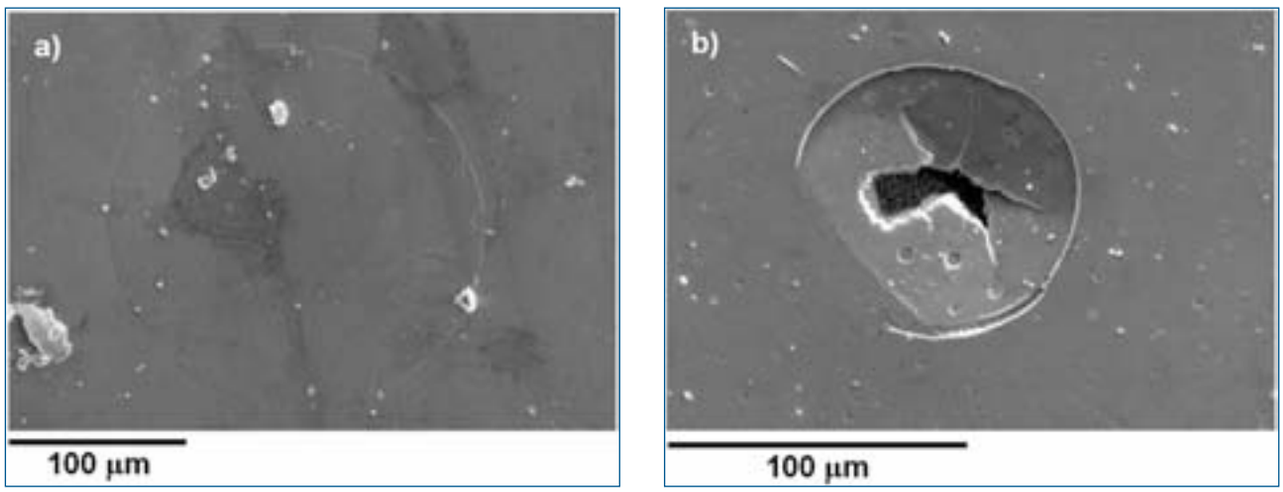

Fig. 11: Corrosion morphology: coating B (a) and coating E (b)

Fig. 11: Morfologie di corrosione per il coating B (a) e per il coating E (b)

The low potential increase and the high reduction of free corrosion current measured in this solution can be explained taking into account the higher efficiency of the cathodic processes that take place on the steel surface in HCl aqueous solution, which probably make almost not influent cathodic reaction on the CrN surface. Based on this hypothesis, the coating acts as a barrier and all cathodic and anodic reactions are therefore localized to the bottom of coating porosities and defects. In fact, only sample D (deposited by CAE) shows a slight increase in the free corrosion potential respect to the bare steel, having on its surface metallic Cr droplets, that can be cathodic respect to the substrate.
These considerations make the mixed potential model not suitable to be used for this environment. Porosity calculated with this method, in fact, is not realistic, being very high and, in many cases, higher than 100% (see Tab. IV).
In this environment, all the analyzed coatings present similar current density and a passive region between 0 and +1000mV; however, their current during passivation is different ($1x10^{-4}$ for the coating E, up to 6 x 10^{-6} for the coating D). As previously seen in NaCl solution, corrosion rate decreases due to the filling of the porosity by corrosion products formed when the material is in the active corrosion range. Current density can be easily related to the calculated porosity level; for high porosity a larger amount of corrosion products (i.e. a higher current density) is needed to occlude porosity and close the access at the solution to the anodic areas.
SEM analyses carried out on the corroded samples show damaging morphology similar to that observed on NaCl corroded samples. On MS coatings pits are present on the surface and cause steel corrosion at the interface coating-substrate. Due to the more aggressive environment on the surface circular areas are visible with a diameter of tens of microns, where the coating was lifted up by the growing corrosion products (Fig. 11a). Sample D surface, on the other hand, is similar to that obtained after NaCl corrosion tests and only Cr droplets appear corroded. This behavior is confirmed also by the low passivity current detected during the test, index of the substrate protection due to the coating.
Samples E show, also in this environment, large areas of delamination affect the second layer of the coating and, differently from NaCl tests, substrate corrosion is present and triggered by the pit presence (Fig. 11b).

CONCLUSIONS

The following conclusions can be drawn from the corrosion experiments carried out on the CrN PVD analyzed in the present paper:

- All the tested coatings protect steel from corrosion in both 3.5wt% NaCl (pH7) solution and 0.1M HCl environment.
- CrN coatings ability to protect tool steel was established to be more pronounced during tests carried out in HCl solution compared to NaCl tests.
- All the coatings have a passivity region extended between 0 and +900mV (SCE) in NaCl environment and from 0 to +1000mV (SCE) in HCl solution.
- Tests carried out in NaCl solution show a good behavior for MS coatings; in particular, the double layer appears as having less porosity respect to the monolayered one and exhibits a lower corrosion current density. CAE samples, on the other hand, have an increased corrosion rate, notwithstanding the lower porosity level, due to the droplets presence.
- Corrosion rates are higher in HCl solution for all the investigated coatings due to the greater chemical aggressiveness of this environment respect to the substrate. Also in this solution the sputtered double layer exhibits the best behavior.
- In HCl solution, corrosion takes place at the interface steel-coating for MS and CAE + MS coatings, starting from a pit that reaches the substrate. CAE samples do not show substrate corrosion but only droplets appear corroded, in the same way as in NaCl environment.
- The deposition of the second layer in CAE + MS coating prevents the contact between metallic droplet and solution, however this coating presents large delamination

areas that make it not suitable to protect the substrate from corrosion in both acid and saline environments.
- The two methods used in porosity calculation have substantial differences. Porosity calculated from Rp agrees with SEM sample observations while mixed potential method gives unreliable values.

ACKNOWLEDGMENTS

This work is supported by REMs project CUP D81J10000220005 financed by Regione Lombardia, moreover, the author are gratefully indebted with Eng. Andrea Ghidini (Lucchini-RS, Lovere) for the steel supply and Eng. Valentina Sisti (TTN, Nerviano) for the CAE coating deposition.

REFERENCES

[1] HUI-PING FENG, CHENG-HSUN HSU, JUNG-KAI LU, YIH-HSUN SHY, Effects of PVD sputtered coatings on the corrosion resistance of AISI 304 stainless steel, Materials Science and Engineering A347 (2003) 123-129.

[2] P.EH. HOVSEPIAN, D.B. LEWIS, W.D. MUNZ, S.B. LYON, M. TOMLINSON, Combined cathodic arc/unbalanced magnetron grown CrN/NbNsuperlattice coatings for corrosion resistant applications, Surface and Coatings Technology 120–121 (1999) 535-541.

[3] FENG CAI, QI YANG, XIAO HUANG, RONGHUA WEI, Microstructure and Corrosion Behavior of CrN and CrSiCN Coatings, JMEPEG (2010) 19:721–727, DOI: 10.1007/s11665-009-9534-3.

[4] L. CHUNA, M. ANDRITSCHKY, L. REBOUTA, R. SILVA, Corrosion of TiN, (TiAl)N and CrN hard coatings producted by magnetron sputtering, Thin Solid Films 317 (1998) 351-355.

[5] Y.H. YOO, J. H. HONG, J.G. KIM, H, Y. LEE, J. G. HAN, Effect of addition Si to CrN coatings on the corrosion resistance of Cr/N stainless steel coating/substrate system in a deareated 3.5wt.% NaCl solution, Surface & Coating Technology 201 (2007) 9518-9523.

[6] J. CREUS, H. MAZILLE, H. IDRISSI, Porosity evaluation of protective coatings onto steel, through electrochemical techniques, Surface and Coatings Technology 130 (2000) 224-232.

[7] M. CĚKADA, P. PANJAN, D. KEK-MERL, M. PANJAN, G. KAPUN, SEM study of defects in PVD hard coatings, Vacuum 82 (2008) 252-256.

[8] P. PANJAN, M. CĚKADA, M. PANJAN, D. KEK-MERL, Growth defects in PVD hard coatings, Vacuum 84 (2010) 209-214.

[9] H.W. WANG, M .M. STACK, S.B. LYONS, P. HOVSEPIANB, W.-D. MIINZ, The corrosion behaviour of macroparticle defects in arc bond-sputtered CrN/NbN superlattice coatings, Surface and Coatings Technology 126 (2000) 279-287.

[10] C. LIU, A. LEYLAND, Q. BI, A. MATTHEWS, Corrosion resistance of multilayered plasma assisted physical vapour deposition TiN and CrN coatings, Surface & Coatings Technology 141 (2001) 164- 173.

[11] M. URGEN, A.F. CAKIR, The effect of heating on corrosion behavior of TiN- and CrN-coated steels, Surface & Coatings Technology 96 (1997) 1236-244.

Effetto del tipo di rivestimento PVD sulla resistenza alla corrosione

Keywords: rivestimenti - corrosione

I rivestimenti sottili PVD sono utilizzati per diverse applicazioni dove sia necessario ottimizzare le proprietà superficiali dei componenti, sia dal punto di vista estetico (coating decorativi) che funzionale (aumento di durezza, resistenza all'abrasione, all'usura e alla corrosione). Nel caso, ad esempio, di stampi per injection moulding, questi sono sollecitati meccanicamente e termicamente dalle pressioni e dalle temperature di processo. Inoltre, sono soggetti a fenomeni di usura causati dello scorrimento del fuso sulle pareti della figura, in modo particolare se si utilizzano polimeri caricati con filler o fibre ad elevata durezza; in aggiunta, possono entrare in contatto con specie chimiche aggressive quali fluoro, zolfo e cloro che vengono rilasciati durante la fase di stampaggio. Il ricorso ad un rivestimento sottile, realizzato in materiale ceramico, comporta sicuramente il duplice vantaggio di poter disporre di uno stampo con durezza superficiale maggiore rispetto al substrato e con reattività chimica inferiore.
Nonostante in letteratura siano presenti diversi lavori sulla caratterizzazione di rivestimenti sottili è difficile trovare un lavoro sistematico che permetta di valutare gli effettivi vantaggi nell'uso di rivestimenti PVD su acciai per stampi.
In questo lavoro si è quindi voluta valutare la resistenza a corrosione di rivestimenti PVD in CrN, mediante prove di polarizzazione elettrochimica in ambiente aggressivo. Sono stati quindi prodotti dei campioni utilizzando due diverse tecniche, DC magnetron sputter (MS) e cathodic arc evaporation (CAE), e si sono considerati cinque gruppi di provini: monostrato e doppio strato sputter (a parità di spessore complessivo), doppio strato depositati tramite arco catodico e, infine, un rivestimento "ibrido" formato da uno strato CAE sul quale è stato depositato un layer MS.
Tutti i rivestimenti sono stati caratterizzati al microscopio elettronico a scansione (SEM) per individuare le differenze tra le diverse tecniche in termini di tipologia e quantità e distribuzione dei difetti presenti. È emerso che i campioni MS presentano una superficie più regolare ma alcune zone risultano danneggiate e con uno spessore di rivestimento inferiore a quello nominale. Al contrario, i coating CAE, a fronte di una superficie più irregolare e caratterizzata da numerose droplet di cromo metallico, non presentano particolari difetti.
Le prove di corrosione elettrochimica sono state svolte in due ambienti contenenti cloruri: il primo neutro (NaCl 3.5% in peso) e il secondo acido (HCl 0.1M) in modo da simulare possibili condizioni critiche di lavoro per gli stampi per l'iniezione dei polimeri. Dai risultati appare chiaramente che i coating formati da due strati sovrappostiti hanno una maggiore resistenza rispetto a quelli monostrato. Al termine dei test sono state ripetute le analisi SEM al fine di correlare il comportamento a corrosione alla tipologia di difetti presenti sul rivestimento.
Infine, è stata calcolata la porosità dei coating, utilizzando i modelli proposti in letteratura, confrontandola con le evidenze sperimentali. Le formule basate sulle resistenze di polarizzazione sono risultate in buon accordo con le analisi morfologiche della superficie dei campioni, al contrario di quanto ottenuto utilizzando il modello del potenziale misto.